



HAL
open science

Genome-wide expression reveals potential biomarkers in breast cancer bone metastasis

Yashbir Singh, Naidu Subbarao, Abhinav Jaimini, Quincy A Hathaway, Amina Kunovac, Bradley Erickson, Vishnu Swarup, Himanshu Narayan Singh

► To cite this version:

Yashbir Singh, Naidu Subbarao, Abhinav Jaimini, Quincy A Hathaway, Amina Kunovac, et al.. Genome-wide expression reveals potential biomarkers in breast cancer bone metastasis. *Journal of Integrative Bioinformatics*, 2022, 19 (3), 10.1515/jib-2021-0041 . hal-03831878

HAL Id: hal-03831878

<https://amu.hal.science/hal-03831878>

Submitted on 27 Oct 2022

HAL is a multi-disciplinary open access archive for the deposit and dissemination of scientific research documents, whether they are published or not. The documents may come from teaching and research institutions in France or abroad, or from public or private research centers.

L'archive ouverte pluridisciplinaire **HAL**, est destinée au dépôt et à la diffusion de documents scientifiques de niveau recherche, publiés ou non, émanant des établissements d'enseignement et de recherche français ou étrangers, des laboratoires publics ou privés.



Distributed under a Creative Commons Attribution 4.0 International License

Yashbir Singh, Naidu Subbarao, Abhinav Jaimini, Quincy A. Hathaway, Amina Kunovac, Bradley Erickson, Vishnu Swarup* and Himanshu Narayan Singh*

Genome-wide expression reveals potential biomarkers in breast cancer bone metastasis

<https://doi.org/10.1515/jib-2021-0041>

Received November 30, 2021; accepted February 8, 2022; published online April 8, 2022

Abstract: Breast cancer metastases are most commonly found in bone, an indication of poor prognosis. Pathway-based biomarkers identification may help elucidate the cellular signature of breast cancer metastasis in bone, further characterizing the etiology and promoting new therapeutic approaches. We extracted gene expression profiles from mouse macrophages from the GEO dataset, GSE152795 using the GEO2R webtool. The differentially expressed genes (DEGs) were filtered by log₂ fold-change with threshold 1.5 (FDR < 0.05). STRING database and Enrichr were used for GO-term analysis, miRNA and TF analysis associated with DEGs. Autodock Vienna was exploited to investigate interaction of anti-cancer drugs, Actinomycin-D and Adriamycin. Sensitivity and specificity of DEGs was assessed using receiver operating characteristic (ROC) analyses. A total of 61 DEGs, included 27 down-regulated and 34 up-regulated, were found to be significant in breast cancer bone metastasis. Major DEGs were associated with lipid metabolism and immunological response of tumor tissue. Crucial DEGs, Bcl3, ADGRG7, FABP4, VCAN, and IRF4 were regulated by miRNAs, miR-497, miR-574, miR-138 and TFs, CCDN1, STAT6, IRF8. Docking analysis showed that these genes possessed strong binding with the drugs. ROC analysis demonstrated Bcl3 is specific to metastasis. DEGs Bcl3, ADGRG7, FABP4, IRF4, their regulating miRNAs and TFs have strong impact on proliferation and metastasis of breast cancer in bone tissues. In conclusion, present study revealed that DEGs are directly involved in of breast tumor metastasis in bone tissues. Identified genes, miRNAs, and TFs can be possible drug targets that may be used for the therapeutics. However, further experimental validation is necessary.

Keywords: biological networking; biomarkers; breast cancer; drug targets; genomics.

*Corresponding authors: Vishnu Swarup, Department of Neurology, All India Institute of Medical Sciences, New Delhi, India, E-mail: vishnuswarup@gmail.com. <https://orcid.org/0000-0003-0759-7818>; and Himanshu Narayan Singh, Aix-Marseille University, INSERM, TAGC, UMR 1090, Marseille 13288, France; and MTA Infotech, Varanasi, India, E-mail: himanshu720@gmail.com. <https://orcid.org/0000-0003-4111-5165>

Yashbir Singh and Bradley Erickson, Department of Radiology, Mayo Clinic, Rochester, MN, USA, E-mail: singh.yashbir@mayo.edu (Y. Singh), bje@mayo.edu (B. Erickson)

Naidu Subbarao, School of Computational and Integrative Sciences, Jawaharlal Nehru University, New Delhi, India, E-mail: nsrao@mail.jnu.ac.in

Abhinav Jaimini, Divisions of PET Imaging, MIRC, Institute of Nuclear Medicine and Allied Sciences (INMAS), Timarpur, Delhi, India

Quincy A. Hathaway, Department of Cardiology, West Virginia University School of Medicine, Heart & Vascular Institute, Morgantown, WV, USA, E-mail: qahathaway@mix.wvu.edu. <https://orcid.org/0000-0001-8226-2319>

Amina Kunovac, Division of Exercise Physiology, West Virginia University School of Medicine, Morgantown, WV, USA, E-mail: ak0086@mix.wvu.edu. <https://orcid.org/0000-0002-5107-3993>

1 Introduction

Worldwide, breast cancer is known to contribute to the highest incidence of cancer-related mortality in women [1]. Metastatic recurrence in breast cancer is associated with poor prognosis and is a leading cause of cancer related death in women worldwide [2]. Despite improved treatments and surgical interventions, about 30% of patients lose their life due to metastasis [3].

Among metastasis in several other tissues and organs in the body (lungs, liver and brain, in addition to lymph nodes), bone is one of the most common sites of invasion in breast cancer [1, 4]. Metastasis to bone typically results in a poor prognosis, reducing life expectancy to 2–3 years post-diagnosis. The tumor cell mass exerts mechanical pressure that can contribute to bone pain. Pain may also occur due to release of inflammatory cytokines from the tumor cells themselves or by altering the bone microenvironment and bone homeostasis in adjacent areas [5].

Bone cancer metastases usually occur in the axial skeleton, in areas with active hematopoiesis and high red marrow content. The microenvironment is fundamental in attracting tumor cells to the bone as well as promoting tumor progression. The composition of the tumor microenvironment changes during tumor development, evolving to meet the demands of the growing neoplasm [6]. These differences affect the progression of cancer and how it responds to therapeutic agents and their ultimate efficacy. An elaborate network of signaling pathways orchestrates the communication between cancer cells and the surrounding stroma. Chemotherapy, radiation therapy, and surgical removal of the tumors are standard methods implemented to cure breast cancers. The usage of thermoset based polymers [7–9] as a drug delivery system is currently a common approach when exploring chemotherapy as an option [10]. Several chemotherapeutic molecules have proven their potential in treatment of breast tumour. Actinomycin D and its analogues and Adriamycin (aka doxorubicin) have been shown to reduce the migration and invasion of tumour cells [11, 12].

In this study, we explore different signaling pathways and associated molecular mechanisms of underlying primary breast cancer development, along with the formation of metastases in the bone. The study will also illustrate biomarkers associated with disease pathophysiology and highlight potential new therapeutics.

2 Materials

The expression profile information of mouse macrophages was extracted from the GEO dataset, GSE152795 (<https://www.ncbi.nlm.nih.gov/geo/query/acc.cgi?acc=GSE152795>). The annotation was performed using Affymetrix GeneChip[®] Mouse Gene 2.0ST Array. The dataset included breast cancer bone metastasis in healthy mouse strains, with a sample size of five in each group. Bone metastasis was generated through intra-cardiac injection of 1×10^5 tumor cells into 4-week-old female mice, while healthy mice were not subjected to intra-cardiac injection.

3 Methods

3.1 Identification of differential expressed genes (DEGs)

The GEO2R (<http://www.ncbi.nlm.nih.gov/geo/geo2r/>) web tool was used to compare mRNA expression between breast cancer metastasis and normal tissue samples in mice. The Benjamini and Hochberg false discovery rate (FDR) method was used to filter out false-positive results, and the adjusted p values were calculated. The differentially expressed genes were filtered based on \log_2 fold change, with a threshold value ≥ 1 and $p < 0.05$. To determine the difference among samples and graphically depict the data, we used a built-in tool of GEO2R Uniform Manifold Approximation and Projection (UMAP). A volcano plot showing differentially expressed genes was constructed using the R Language ggplot package.

The receiver operating characteristics (ROC) curve was plotted to determine the specificity and sensitivity of the identified DEGs towards controls and tumor samples using Stata v17.0. The statistical significance level was established as p value < 0.05 .

3.2 Network analysis

The protein network analysis of the differentially expressed genes was performed using the STRING database (<http://string-db.org>), which provides a physical and functional association of proteins. It also provides information about how genes are enriched via various pathways. The functional and pathway enrichment analyses were performed with the cut-off criterion p -value < 0.05 . Protein-protein interaction visualization was done through the STRING database.

3.3 Identification of transcription factors and miRNAs binding to DEGs

The Enrichr webtool [13] was exploited to extract miRNA targeting the identified genes. Significantly ($p < 0.05$) enriched miRNAs were extracted. The information on protein-protein interactions (PPI) of TFs was also fetched from the Enrichr webtool.

3.4 Molecular docking

3.4.1 Protein preparation: The 3D structure of the targets FABP4 (PDB ID: 3P6D) and IRF4 (PDB ID: 7JM4) were extracted from the Protein Databank. The protein structure of ADGRG7 was extracted from the AlphaFold Protein Structure Database (<https://alphafold.ebi.ac.uk/entry/Q96K78>). Local minimization of the structure was done by the GROMOS96 (43B1 parameter set) and the Swiss-pdbViewer used for implementation [14]. The CASTp (Computed Atlas of Surface Topography of proteins) web tool was used to extract ligand binding site information [15].

3.4.2 Preparation of ligand molecules: The three-dimensional structure of the drugs, Actinomycin D (PubChem ID: 31703) and Adriamycin (PubChem ID: 457193), were extracted from the PubChem database [16]. The ligand structures were converted to pdbqt format by OpenBabel software [17].

3.4.3 Binding in silico: The protein preparation in pdbqt-format was executed using AutodockTools 1.5.4 suite [18]. The molecular docking analysis was performed to develop an improved modeled structure by Autodock Vina Software [19]. After docking analysis, the obtained structures were detected by the Protein-Ligand Interaction Profiler (PLIP) web server (Technical University of Dresden) and tabularized for further analysis [20].

Figure 1 presents an overview of methods used in present differential expression analysis of macrophages of healthy bone & breast cancer bone metastasis.

4 Results

4.1 Sample relatedness

The sample and group relationships were identified using the Uniform Manifold Approximation and Projection (UMAP) dimension reduction technique; this provided clustering of the tumor and normal tissues into their respective groups. By color-coding of the sample group on the UMAP, we observed a clear difference between the cancer metastasis group and that of the controls, as shown in Figure 2A, where green depicts the breast cancer bone metastasis samples, and healthy samples are shown in blue-grey.

4.2 Differentially expressed genes

A total of 61 genes were found to be significantly differentially expressed in breast cancer bone metastasis. This included 27 down-regulated genes shown in blue, and 34 up-regulated genes depicted in red (Figure 2B, Supplementary Table S1). Two genes found to be up-regulated by greater than a factor of 3 were Saa3 (Serum amyloid A-3 protein) and Lipg (Supplementary Table S1). They were found to be directly correlated with breast cancer. A new gene, LIPG, was recently found to express and play a role in breast cancer proliferation, tumorigenicity, and metastasis [21]. An acute-phase protein produced by hepatocytes and adipose tissues named Serum amyloid A (SAA) binds to pattern recognition receptors (PRRs), and has a potential role in tumor promotion [22].

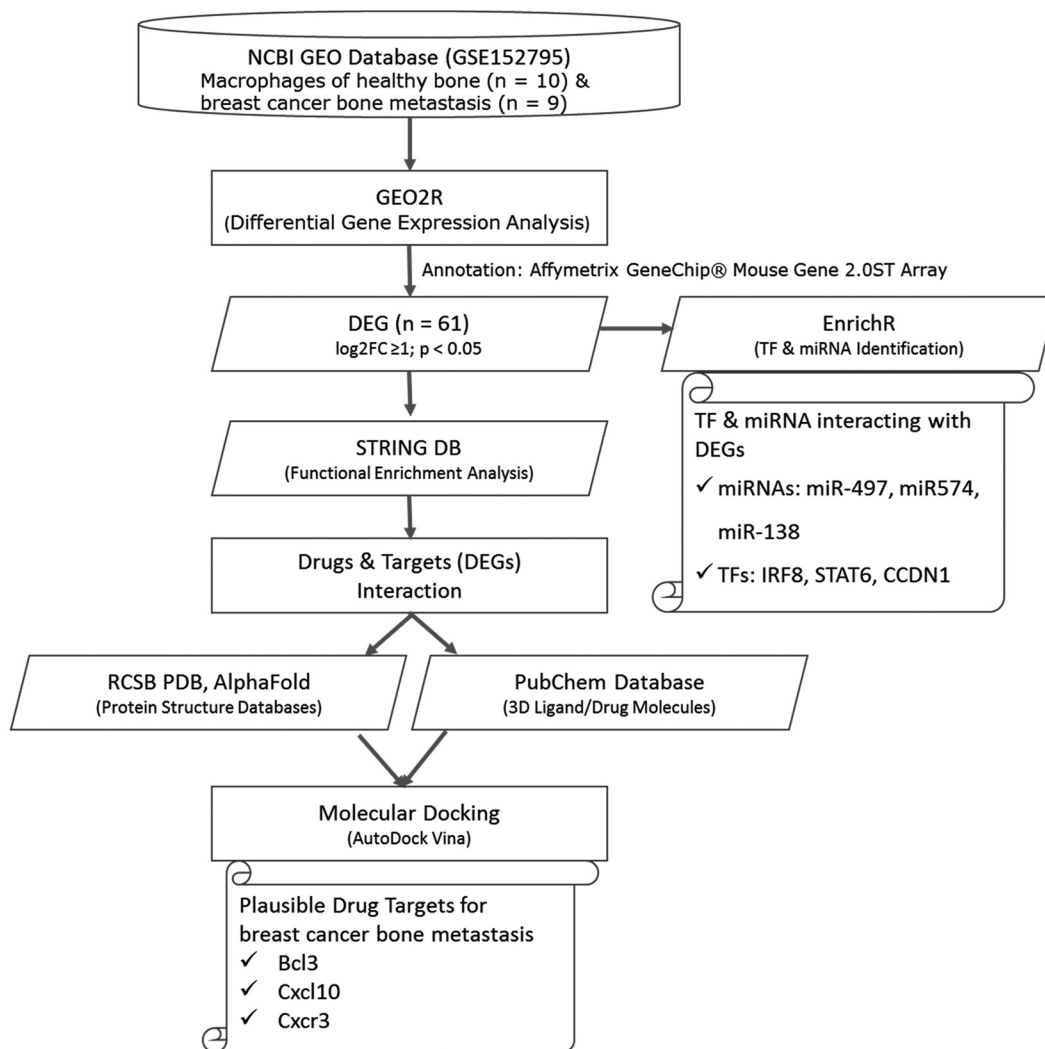


Figure 1: The overall workflow of the methods employed in identifying drug targets, TFs and miRNAs.

4.3 Functional enrichment analysis

Our results demonstrate that a total of 122 and 105 GO-terms were found to be significantly ($FDR < 0.05$) enriched for up-regulated genes and down-regulated genes, respectively (Supplementary Tables S2, S3). The top 20 biological processes highly enriched differentially expressed genes were found to be associated with immunological activation and lipid metabolism (Figure 3). The differentially expressed genes were found to be significantly associated with receptor activity and/or binding functions. The differentially expressed genes were major components of the cell membrane or extracellular membrane. Out of 34 up-regulated genes, only 19 genes were found to be associated with the top 20 enriched biological processes that were related to immunological responses. However, 21 down-regulated genes were enriched in the top 20 biological processes associated with lipid metabolism and immunological responses (Supplementary Table S2, S3).

4.4 TFs and miRNAs binding to DEGs

The Enrichr identified 28 miRNAs (Supplementary Table S4) which are targeting DEGs. The miRNA-mRNA interaction map, made by using miRNet v2.0 showed seven of these DEGs having strong interactions with

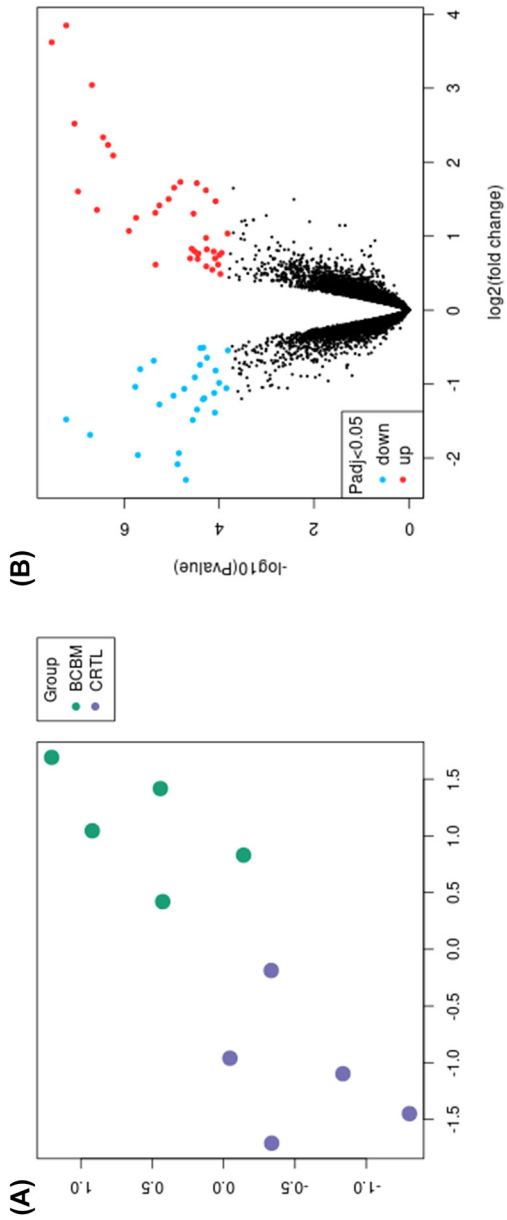


Figure 2: Identification of differentially expressed genes. (A) Uniform manifold approximation and projection (UMAP) plot shows sample relatedness. Healthy bone samples are shown in blue-grey and cancer samples are shown in green. (B) Volcano plot is showing differentially expressed genes. Red color: upregulated genes ($\log_{2}FC > 1$ and $\text{padj} < 0.05$). Blue shows: downregulated genes ($\log_{2}FC < -1$ and $\text{padj} < 0.05$). Gray color denotes no significant change in the expression.

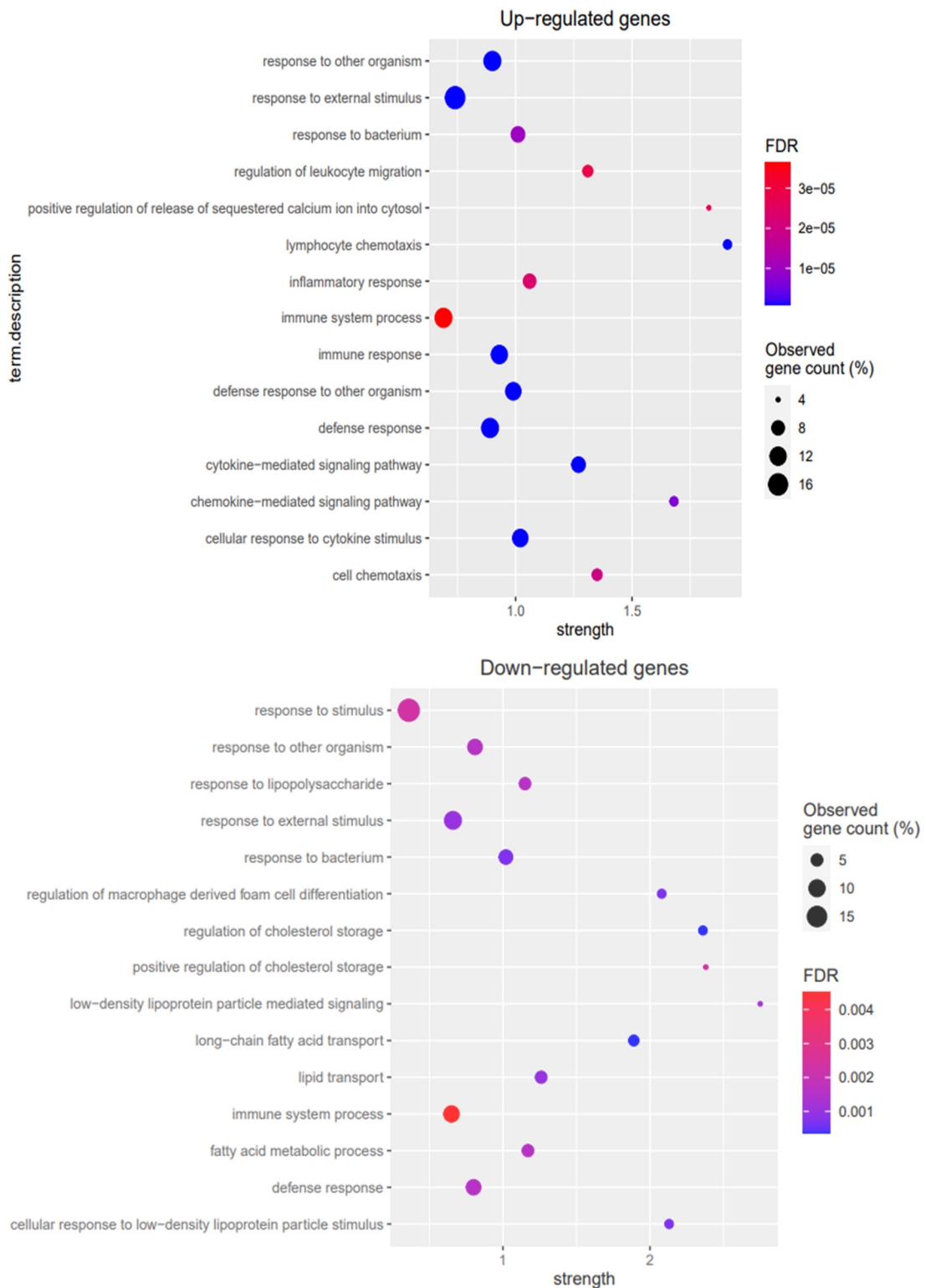


Figure 3: Bubble plot of the GO analysis of DEGs. The top 20 items of 'biological process' in upregulated genes (upper panel) and downregulated genes (lower panel) were displayed with the parameters strength and $-\log_{10} p$ -value. Strength: $\log_{10}(\text{observed}/\text{expected})$. This measure describes how large the enrichment effect is. It is the ratio between (i) the number of proteins in your network that are annotated with a term and (ii) the number of proteins that we expect to be annotated with this term in a random network of the same size.

miRNAs (Figure 4). Genes IRF4 and VCAN showed the highest degree of interactions while MRC1 showed the least level of interaction.

Seven significant TFs ($p < 0.05$) were identified by Enrichr (Figure 5A, Supplementary Table S5). The interactions of these TFs with other proteins/TFs in Figure 5B clearly show strong interaction. The interaction between TFs showed PRDM1 connected with various other TFs which depicted its central role in pathogenesis (Figure 5B).

4.5 ROC analysis

In the Bcl3 gene, the fitted ROC curve is estimated with the assumption of binomial distribution (Figure 6). The parametric estimate of the area under the fitted ROC curve was 0.92 and its 95% confidence interval are 0.73972 and 0.99867. Only the Bcl3 gene showed significant relevance with sensitivity and specificity with the disease as compared to other genes (Supplementary Figure S1A–H).

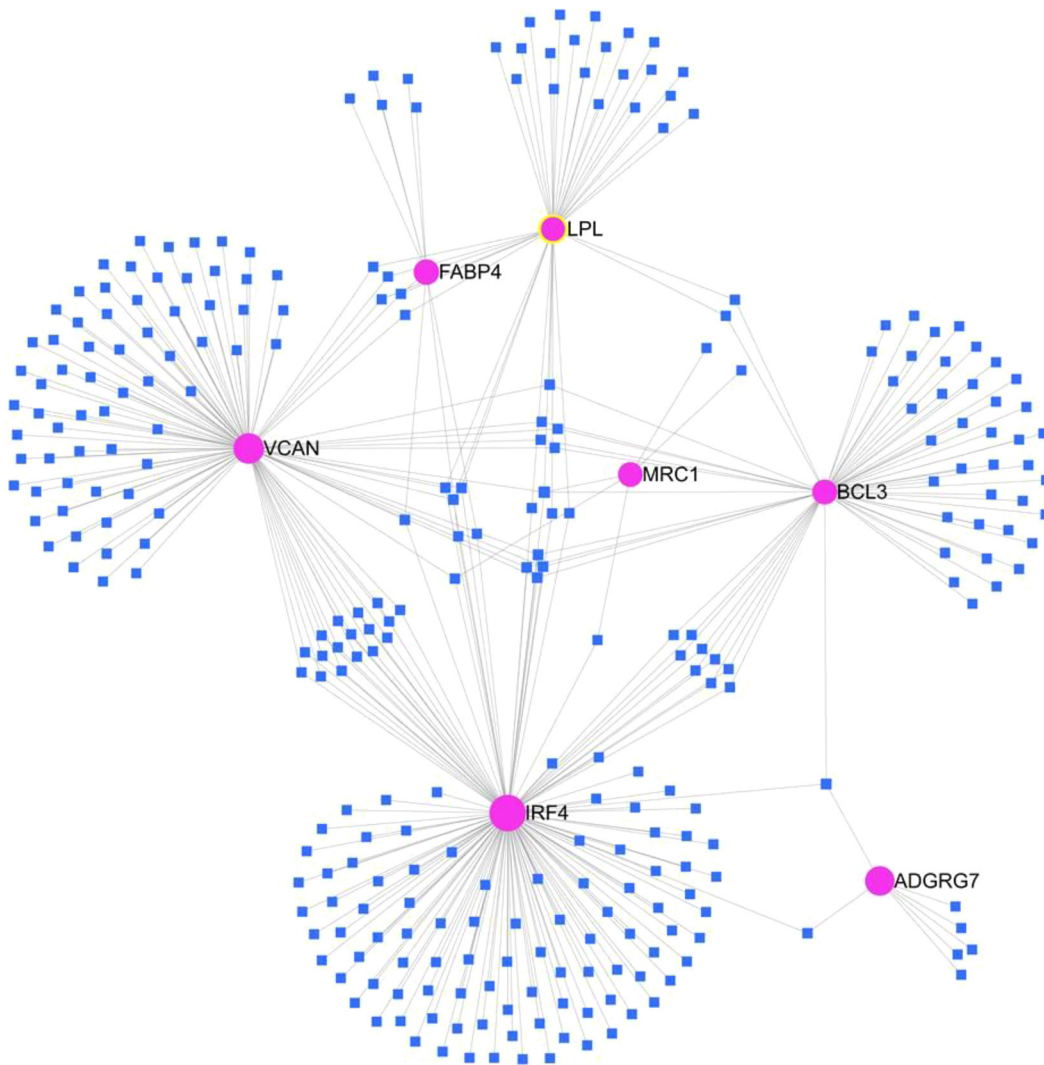


Figure 4: Network of identified miRNAs and their target genes made by miRNet 2.0. The round pink spots represent DEGs and the blue coloured squares represent the miRNAs.

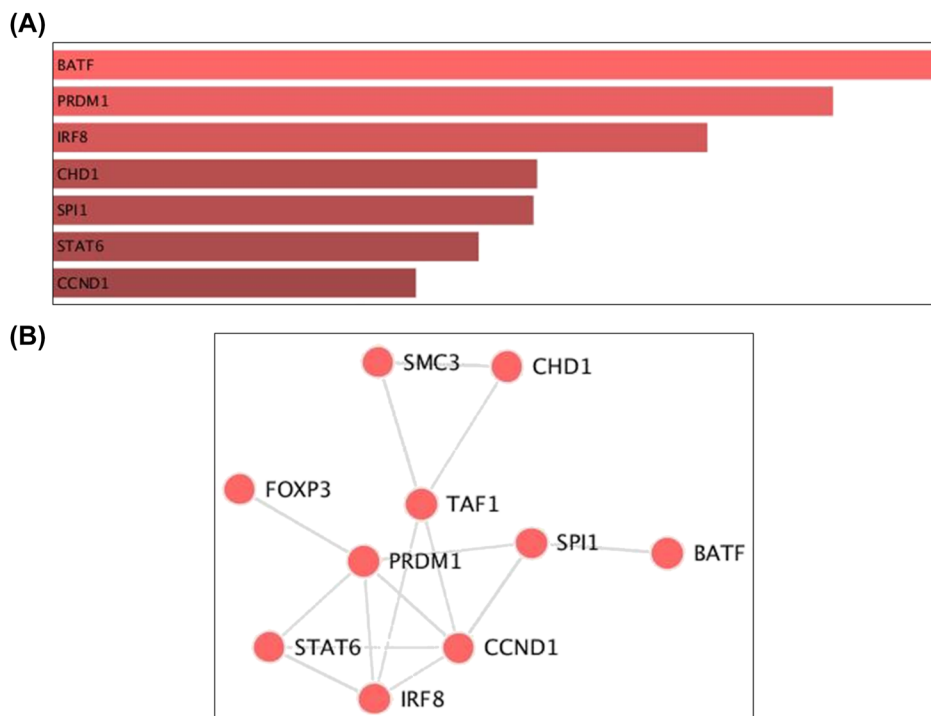


Figure 5: Identified significant TFs targeting DEGs and their interaction with other TFs/proteins.

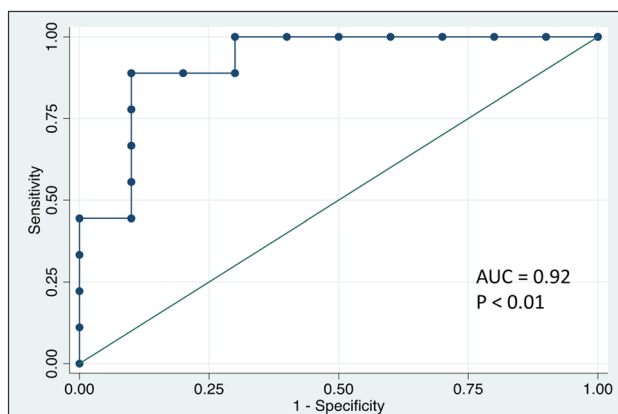


Figure 6: ROC curve analysis to test the validity of Bcl3 gene expression in discriminating samples of patients and controls.

4.6 Interaction of DEGs and most common drugs used in treatment

The binding site for the target proteins ADGRG7, FABP4 and IRF4 were predicted to be located around ILE (Chain A; Sequence ID: 34), PHE (Chain A; Sequence ID: 16) and GLY (Chain G; Sequence ID: 22), respectively (Figure 7 A–C, Supplementary Table S7–S9). The molecular docking interaction analysis of Actinomycin and Adriamycin drugs, with all the protein targets showed high binding energy (Table 1).

The free binding energies of the molecules were found to be ranged from -7.6 to -9.4 kcal/mol. The protein-ligand complex of ADGRG7 with both drugs was observed with the highest binding energy (ADGRG7-Actinomycin complex $\Delta G = -9.4$ kcal/mol; ADGRG7-Adriamycin complex $\Delta G = -8.1$ kcal/mol). The free binding energy of ADGRG7-Actinomycin complex was highest (-9.4 kcal/mol) and the IRF4-Adriamycin complex showed lowest binding energy of (-7.6 kcal/mol).

post-follow-up [25]. Tumor cells regulate several factors in the bone microenvironment for their maintenance and growth. By releasing cytokines, chemokines, and growth factors, the bone microenvironment inhibits colonization of cancer cells in healthy bones, or supports colonization in cancerous conditions [26, 27]. Production of interferon- γ (IFN- γ) by activated CD4 + T cells inhibits osteoclasts' activity, thereby protecting bone [28]. Whereas after tumor cell invasion, osteoclastogenesis is promoted by the release of osteoprotegerin (OPG) and cytokines (IL6, IL15 etc.), leading to bone destruction [29]. Thus, an altered balance within the immune system between pro-tumorigenic and anti-tumorigenic molecules decides the fate of tumor cells in bone.

In addition, immune cell plasticity has extensive implications in the pathogenesis and resolution of metabolic disorders: cancers, autoimmune diseases, and chronic inflammatory disorders. In metabolic disorders such as obesity, immune cells interact with various classes of lipids, which can control the plasticity of macrophages and T-lymphocytes. Alterations in lipid metabolism are directly associated with immune cell activation and are also involved in mechanisms associated with several human diseases such as cancer [30]. The proliferation of tumor cells and metastases requires a large amount of energy which is obtained by alterations in lipid metabolism [31]. Several clinical studies have demonstrated high levels of lipids (triglycerides, high density- and low density lipoproteins) in blood plasma of breast cancer patients [32]. Moreover, accumulation of these molecules was correlated with a high propensity of metastases in breast cancer patients. Elevated free fatty acid levels also inhibit fibrin degradation, facilitating breast cancer invasion and metastasis [33]. Thus, a dysregulated immune system and lipid metabolism promote metastases in breast cancer.

This study demonstrates that the up-regulated genes in breast cancer metastases are found to be associated with immune responses. On the other hand, down-regulated genes were involved with the immune response as well as lipid metabolism biological processes (Figure 3).

Four-fold down-regulation of the platelet glycoprotein *Cd36* was observed in mouse macrophages of breast cancer bone metastases samples (Table S1). The *Cd36* down-regulation was also observed in primary tumor epithelium, and its possible association with breast cancer metastases was reported [34, 35]. Peroxisome proliferator-activated receptor-gamma (*PPAR- γ*) is a nuclear hormone receptor superfamily transcription factor involved in metabolic functions as well as a suppressor of breast cancer tumors [36] and was estimated to be down-regulated two-fold in tumors. Similarly, other downregulated genes (*Fabp4*, *Mrc1*, *Lpl*, *Cd209d*, and *Cd209a*) were also found to be involved in breast cancer and may be associated with bone metastases. However, further investigation is required to confirm their association with bone metastases. Lipoprotein lipase (*Lpl*) was observed to be depleted in the disease condition (Table S1). *Lpl* functions as a triglyceride hydrolase and receptor-mediated factor for lipoprotein uptake [37]. Loss of *Lpl* expression was reported to be directly associated with lipid metabolism and to cause hyperlipidemia [38, 39]. A previous study suggests that down-regulation of *Lpl* may be the result of epigenetic alterations, such as CpG island hypermethylation and/or histone modification [40]. Altered genomic DNA is also reported to contribute to the loss of *Lpl*. The cancer susceptibility gene deleted in breast cancer (*Dcb2*), known as Rho-related BTB domain containing 2 (*Rohbtb2*), mapped closed to the *Lpl* gene which may also be affected by *Lpl* deletion and could therefore exert a combined impact on promoting carcinogenesis [40, 41]. *Lpl* is found to suppress TNF α and IFN γ associated inflammation activating genes through inactivation of transcription factor NF- κ B [40, 42]. Therefore, loss of *Lpl* activity may promote carcinogenesis.

Several significantly up-regulated genes were identified in the macrophages in the cancer phenotype. One of the up-regulated genes, *Bcl3* was found to be approximately two and a half times higher than the controls. It is a transcription co-activator proto-oncogene and a candidate for therapeutic intervention of disease progression. *Bcl3* is aberrantly expressed in tumors, including breast cancer. Although the role of *Bcl3* in tumor pathology is poorly understood, it mediates transcription suppression of NF- κ B signaling and affects metastasis-associated genes. *Bcl3* deficiency was found with only minor immunologic defects. Therefore, it may also be considered a plausible drug target [43]. Interleukin-1 receptor type 2 (*IL1R2*), was discovered to be a negative immune regulator, and is three-fold up-regulated in pathologic cases (Table S1). *IL1R2* binds and increases the activity of the ubiquitin-specific protease 15 (*USP15*) in breast cancer cells. *IL1R2* promotes the self-renewal of breast tumor-initiating cells, as well as cancer proliferation and invasion

[44]. However, USP15 is a deubiquitinase and was found to be involved in several cellular signaling pathways such as COP9-signalosome, NF κ B, and p53 signaling pathways [45]. The *in vitro* and *in vivo* study suggested that overexpression of IL1R2 leads to down-regulation of USP15, and helps in controlling breast cancer malignancy. Therefore, IL1R2 was reported to be a potential therapeutic target for breast cancer treatment [44]. Additionally, the cytokines and chemokines (Cxcl10, Cxcl9, and Cxcr3) were found to be up-regulated (Table S1) in the phenotype. These factors are suggested to play a role in driving cancer cell proliferation in the bone microenvironment [46].

Further, the extended analysis using Enrichr showed several crucial miRNAs like miR-138-5p, miR-26a-5p, miR-574-5p, hsa-miR-331-5p (Supplementary Table S4) which are targeting to DEGs. The miR-138-5p and miR-331 are associated with cell migration and invasion ability of breast cancer cells [47–49]. The miR-497 suppresses proliferation and induces apoptosis in breast cancer cells by targeting Bcl-w gene [50]. The miR-26a-5p is a well known tumor oncogene for osteosarcoma [51] and is also known to inhibit breast cancer cell growth [52]. The miR-26a-5p was found to be remarkably upregulated in osteosarcoma patients and significantly correlated with poor prognosis [53]. The miR-574-5p was found to be highly related to development and metastasis of breast cancer [54]. It was reported actively involved in the Wnt/ β -catenin signaling pathway and plays crucial role in bone metastasis in non-small cell lung cancer (NSCLC) patients [55]. These miRNAs target identified DEGs which is evident from Figure 4 and Supplementary Table S4 and their interaction have been proven experimentally in literature. The miR-497 suppresses proliferation and induces apoptosis in breast cancer cells by targeting Bcl-w gene [50].

The Enrichr also showed several significant TFs ($p < 0.05$) which are interacting with identified DEGs (Supplementary Table S5, Figure 5A). The IRF8 (Interferon regulatory factor 8) and BATF (Basic Leucine Zipper ATF-Like Transcription Factor) are very crucial in developing the anti-tumour response in tumour surveillance. IRF and BATF negative mice had a fast rate of tumour development [56, 57]. Notably, these TFs and other TFs like STAT6 and CCDN1 are directly involved in developing breast cancer and its metastasis [58–60]. Deregulated levels of these TFs are correlated with unfavorable relapse-free survival of patients. The ROC analysis showed that Bcl3 gene possessed highest specificity and sensitivity to distinguish cancer and control samples while other identified genes failed to correlate with that (Figure 6, Supplementary Figure S1A–H, supplementary Table S6).

Selected genes were analysed for their binding to most common anti-tumour drugs (Actinomycin-D and Adriamycin) by molecular docking (Figure 7, Supplementary Table S7–S9). The Actinomycin-D (Act-D) is a well-known potent anticancer drug produced by Streptomyces bacteria. The high toxicity caused by Act-D is attributed to its ability to inhibit transcription of several important gene such as c-myc, c-met, myotonic Dystrophy type 1 etc. Importantly, it has been approved by the FDA for multiple tumors, Wilms' tumor and gestational choriocarcinoma and in combination with other drugs to treat high risk tumor in chemotherapy regime [61–63]. The chemical structure of Act-D comprises planar phenoxazone ring and two cyclic pentapeptide lactones, a very heavy molecule [63]. The Adriamycin (synonym doxorubicin) is a glycoside antibiotic whose structure and stereochemistry are represented in Figure 6 (formula I). It consists of the tetracyclic quinoid aglycone adriamycinone (14-hydroxydaunomycinone) linked to the aminosugar daunosamine [64, 65]. Both drugs were found to bind selected genes (ADGRG7, FABP4, IRF4) efficiently (free energy $-7.6-9.4$ kcal/mol; Table 1).

The study unveiled various deregulated genes demonstrating a strong role in bone metastasis of breast cancer macrophages. Distinct and altered signaling pathways were identified and it was determined that their key genes are likely involved in promoting carcinogenesis. Deregulated genes in lipid metabolism are directly involved in immunological responses, which in turn promote cancer and its spread to bone. The molecular docking study revealed that the identified deregulated genes (ADGRG-7 and IRF4) have vital anticancer drugs (Actinomycin-D and Adriamycin) targets. ROC analysis showed BCL3 gene was most specific with breast cancer-associated bone metastasis. The extended analysis by Enrichr identified miRNAs and TFs which are directly involved in the crucial pathological mechanism. However, their exact role in the pathophysiology of bone metastasis needs to be investigated within *in vitro* conditions.

6 Conclusions

In breast cancer bone metastasis, most immunological molecules such as chemokines, cytokines, and lipid metabolism molecules were found to be altered. These identified altered pathways promote bone metastasis outgrowth and prolonged survival of tumor cells. Some of the up-regulated genes such as Bcl3, Cxcl10, and Cxcr3; miRNAs (miR-497, miR-574, miR-138) and TFs (IRF8, STAT6, CCDN1) associated with metastasis may also be plausible targets for future therapeutics. However, *in vitro* and *in vivo* studies are required to confirm the role of these identified genes and pathways in the pathogenesis.

Author contribution: All authors wrote the paper and critically commented to the manuscript. All authors read and approved the final manuscript.

Research funding: None declared.

Conflict of interest statement: There are no conflicts of interest.

References

- Pan Y, Lin Y, Mi C. Clinicopathological characteristics and prognostic risk factors of breast cancer patients with bone metastasis. *Ann Transl Med* 2021;9:1340.
- Siegel RL, Miller KD, Jemal A. Cancer statistics. *CA A Cancer J Clin* 2020;70:7–30.
- Caswell-Jin JL, Plevritis SK, Tian L, Cadham CJ, Xu C, Stout NK, et al. Change in survival in metastatic breast cancer with treatment advances: meta-analysis and systematic review. *JNCI Cancer Spectr* 2018;2:pk062.
- Pulido C, Vendrell I, Ferreira AR, Casimiro S, Mansinho A, Alho I, et al. Bone metastasis risk factors in breast cancer. *Ecancermedalscience* 2017;11:715.
- Macedo F, Ladeira K, Pinho F, Saraiva N, Bonito N, Pinto L, et al. Bone metastases: an overview. *Onco Rev* 2017;11:321.
- Hanahan D, Weinberg RA. Hallmarks of cancer: the next generation. *Cell* 2011;144:646–74.
- Patel JP, Deshmukh S, Zhao C, Wamuo O, Hsu SL, Schoch AB, et al. An analysis of the role of nonreactive plasticizers in the crosslinking reactions of a rigid resin. *J Polym Sci B Polym Phys* 2017;55:206–13.
- Patel JP, Xiang ZG, Hsu SL, Schoch AB, Carleen AA, Matsumoto D. Path to achieving molecular dispersion in a dense reactive mixture. *J Polym Sci B Polym Phys* 2017;53:1519–26.
- Xu D, Wang H-W, Patel J, Brun XF, Hirota K, Capsuto E, et al. A novel design of temporary Bond debond adhesive technology for wafer-level assembly. In: 2020 IEEE 70th Electronic Components and Technology Conference (ECTC); 2020. pp. 68–74.
- Sharma A, Jain N, Sareen R. Nanocarriers for diagnosis and targeting of breast cancer. *BioMed Res Int* 2013;2013:960821.
- Salerno M, Cenni E, Fotia C, Avnet S, Granchi D, Castelli F, et al. Bone-targeted doxorubicin-loaded nanoparticles as a tool for the treatment of skeletal metastases. *Curr Cancer Drug Targets* 2010;10:649–59.
- Lin S, Zhang C, Liu F, Ma J, Jia F, Han Z, et al. Actinomycin V inhibits migration and invasion via suppressing snail/slug-mediated epithelial-mesenchymal transition progression in human breast cancer MDA-MB-231 cells in vitro. *Mar Drugs* 2019;305. <https://doi.org/10.3390/md17050305>.
- Chen EY, Tan CM, Kou Y, Duan Q, Wang Z, Meirelles GV, Clark NR, Ma'ayan A. Enrichr: interactive and collaborative HTML5 gene list enrichment analysis tool. *BMC Bioinf* 2013;14:128.
- Johansson MU, Zoete V, Michielin O, Guex N. Defining and searching for structural motifs using DeepView/Swiss-PdbViewer. *BMC Bioinf* 2012;13:173.
- Tian W, Chen C, Lei X, Zhao J, Liang J. CASTp 3.0: computed atlas of surface topography of proteins. *Nucleic Acids Res* 2018;46:W363–7.
- Kim S, Chen J, Cheng T, Gindulyte A, He J, He S, et al. PubChem in 2021: new data content and improved web interfaces. *Nucleic Acids Res* 2021;49:D1388–95.
- O'Boyle NM, Banck M, James CA, Morley C, Vandermeersch T, Hutchison GR. Open Babel: an open chemical toolbox. *J Cheminf* 2011;3:33.
- Morris GM, Huey R, Lindstrom W, Sanner MF, Belew RK, Goodsell DS, et al. AutoDock4 and AutoDockTools4: automated docking with selective receptor flexibility. *J Comput Chem* 2009;30:2785–91.
- Trott O, Olson AJ. AutoDock Vina: improving the speed and accuracy of docking with a new scoring function, efficient optimization, and multithreading. *J Comput Chem* 2010;31:455–61.
- Salentin S, Schreiber S, Haupt VJ, Adasme MF, Schroeder M. PLIP: fully automated protein-ligand interaction profiler. *Nucleic Acids Res* 2015;43:W443–447.

21. Cadenas C, Vosbeck S, Edlund K, Grgas K, Madjar K, Hellwig B, et al. LIPG-promoted lipid storage mediates adaptation to oxidative stress in breast cancer. *Int J Cancer* 2019;145:901–15.
22. Fourie C, Shridas P, Davis T, de Villiers WJS, Engelbrecht A-M. Serum amyloid A and inflammasome activation: a link to breast cancer progression? *Cytokine Growth Factor Rev* 2021;59:62–70.
23. Manders K, van de Poll-Franse LV, Creemers G-J, Vreugdenhil G, van der Sangen MJC, Nieuwenhuijzen GAP, et al. Clinical management of women with metastatic breast cancer: a descriptive study according to age group. *BMC Cancer* 2006;6:179.
24. Kennecke H, Yerushalmi R, Woods R, Cheang MCU, Voduc D, Speers CH, et al. Metastatic behavior of breast cancer subtypes. *J Clin Oncol* 2010;28:3271–7.
25. Liede A, Jerzak KJ, Hernandez RK, Wade SW, Sun P, Narod SA. The incidence of bone metastasis after early-stage breast cancer in Canada. *Breast Cancer Res Treat* 2016;156:587–95.
26. Peinado H, Zhang H, Matei IR, Costa-Silva B, Hoshino A, Rodrigues G, et al. Pre-metastatic niches: organ-specific homes for metastases. *Nat Rev Cancer* 2017;17:302–17.
27. Sceneay J, Smyth MJ, Möller A. The pre-metastatic niche: finding common ground. *Cancer Metastasis Rev* 2013;32:449–64.
28. Xu Z, Hurchla MA, Deng H, Uluçkan O, Bu F, Berdy A, et al. Interferon-gamma targets cancer cells and osteoclasts to prevent tumor-associated bone loss and bone metastases. *J Biol Chem* 2009;284:4658–66.
29. Sawant A, Hensel JA, Chanda D, Harris BA, Siegal GP, Maheshwari A, et al. Depletion of plasmacytoid dendritic cells inhibits tumor growth and prevents bone metastasis of breast cancer cells. *J Immunol (Baltimore, Md: 1950)* 2012;189:4258–65.
30. Hubler MJ, Kennedy AJ. Role of lipids in the metabolism and activation of immune cells. *J Nutr Biochem* 2016;34:1–7.
31. Zhu Y, Aupperlee MD, Zhao Y, Tan YS, Kirk EL, Sun X, et al. Pubertal and adult windows of susceptibility to a high animal fat diet in Trp53-null mammary tumorigenesis. *Oncotarget* 2016;7:83409–23.
32. Wei LJ, Zhang C, Zhang H, Wei X, Li SX, Liu JT, et al. A case-control study on the association between serum lipid level and the risk of breast cancer. *Zhonghua Yu Fang Yi Xue Za Zhi [Chinese Journal of Preventive Medicine]* 2016;50:1091–5.
33. Byon CH, Hardy RW, Ren C, Ponnazhagan S, Welch DR, McDonald JM, et al. Free fatty acids enhance breast cancer cell migration through plasminogen activator inhibitor-1 and SMAD4. *Lab Invest* 2009;89:1221–8.
34. Johnstone CN, Smith YE, Cao Y, Burrows AD, Cross RSN, Ling X, et al. Functional and molecular characterisation of EO771.LMB tumours, a new C57BL/6-mouse-derived model of spontaneously metastatic mammary cancer. *Dis Models Mech* 2015;8:237–51.
35. Enciu A-M, Radu E, Popescu ID, Hinescu ME, Ceafalan LC. Targeting CD36 as biomarker for metastasis prognostic: how far from translation into clinical practice? *BioMed Res Int* 2018;2018:7801202.
36. Rovito D, Gionfriddo G, Barone I, Giordano C, Grande F, De Amicis F, et al. Ligand-activated PPAR γ downregulates CXCR4 gene expression through a novel identified PPAR response element and inhibits breast cancer progression. *Oncotarget* 2016;7:65109–24.
37. Miller AL, Smith LC. Activation of lipoprotein lipase by apolipoprotein glutamic acid. Formation of a stable surface film. *J Biol Chem* 1973;248:3359–62.
38. Gehrlich S. Common mutations of the lipoprotein lipase gene and their clinical significance. *Curr Atherosclerosis Rep* 1999;1:70–8.
39. Mead JR, Irvine SA, Ramji DP. Lipoprotein lipase: structure, function, regulation, and role in disease. *J Mol Med* 2002;80:753–69.
40. Takasu S, Mutoh M, Takahashi M, Nakagama H. Lipoprotein lipase as a candidate target for cancer prevention/therapy. *Biochem Res Int* 2012;2012:398697.
41. Knowles MA, Aveyard JS, Taylor CF, Harnden P, Bass S. Mutation analysis of the 8p candidate tumour suppressor genes DBC2 (RHOBTB2) and LZTS1 in bladder cancer. *Cancer Lett* 2005;225:121–30.
42. Kota RS, Ramana CV, Tenorio FA, Enelow RI, Rutledge JC. Differential effects of lipoprotein lipase on tumor necrosis factor-alpha and interferon-gamma-mediated gene expression in human endothelial cells. *J Biol Chem* 2005;280:31076–84.
43. Schwarz EM, Krimpenfort P, Berns A, Verma IM. Immunological defects in mice with a targeted disruption in Bcl-3. *Genes Dev* 1997;11:187–97.
44. Zhang L, Qiang J, Yang X, Wang D, Rehman AU, He X, et al. IL1R2 blockade suppresses breast tumorigenesis and progression by impairing USP15-dependent BMI1 stability. *Adv Sci* 2020;7:1901728.
45. Chou C-K, Chang Y-T, Korinek M, Chen Y-T, Yang Y-T, Leu S, et al. The regulations of deubiquitinase USP15 and its pathophysiological mechanisms in diseases. *Int J Mol Sci* 2017;18:E483.
46. Romero-Moreno R, Curtis KJ, Coughlin TR, Miranda-Vergara MC, Dutta S, Natarajan A, et al. The CXCL5/CXCR2 axis is sufficient to promote breast cancer colonization during bone metastasis. *Nat Commun* 2019;10:4404.
47. Zhao C, Ling X, Li X, Hou X, Zhao D. MicroRNA-138-5p inhibits cell migration, invasion and EMT in breast cancer by directly targeting RHBDD1. *Breast Cancer* 2019;26:817–25.

48. Karagkouni D, Paraskevopoulou MD, Chatzopoulos S, Vlachos IS, Tastsoglou S, Kanellos I, et al. DIANA-TarBase v8: a decade-long collection of experimentally supported miRNA-gene interactions. *Nucleic Acids Res* 2018;46:D239–45.
49. McAnena P, Tanriverdi K, Curran C, Gilligan K, Freedman JE, Brown JAL, et al. Circulating microRNAs miR-331 and miR-195 differentiate local luminal a from metastatic breast cancer. *BMC Cancer* 2019;19:436.
50. Shen L, Li J, Xu L, Ma J, Li H, Xiao X, et al. MiR-497 induces apoptosis of breast cancer cells by targeting Bcl-w. *Exp Ther Med* 2012;3:475–80.
51. Yu T, Chen D, Zhang L, Wan D. MicroRNA-26a-5p promotes proliferation and migration of osteosarcoma cells by targeting HOXA5 in vitro and in vivo. *OncoTargets Ther* 2019;12:11555–65.
52. Huang Z-M, Ge H-F, Yang C-C, Cai Y, Chen Z, Tian W-Z, et al. MicroRNA-26a-5p inhibits breast cancer cell growth by suppressing RNF6 expression. *Kaohsiung J Med Sci* 2019;35:467–73.
53. Xie X-Y, Chen X-M, Shi L, Liu J-W. Increased expression of microRNA-26a-5p predicted a poor survival outcome in osteosarcoma patients: an observational study. *Medicine* 2021;100: e24765.
54. Wang P-S, Chou C-H, Lin C-H, Yao Y-C, Cheng H-C, Li H-Y, et al. A novel long non-coding RNA linc-ZNF469-3 promotes lung metastasis through miR-574-5p-ZEB1 axis in triple negative breast cancer. *Oncogene* 2018;37:4662–78.
55. Yang X-R, Pi C, Yu R, Fan X-J, Peng X-X, Zhang X-C, et al. Correlation of exosomal microRNA clusters with bone metastasis in non-small cell lung cancer. *Clin Exp Metastasis* 2021;38:109–17.
56. Hildner K, Edelson BT, Purtha WE, Diamond M, Matsushita H, Kohyama M, et al. Batf3 deficiency reveals a critical role for CD8alpha + dendritic cells in cytotoxic T cell immunity. *Science (New York, N.Y.)* 2008;322:1097–100.
57. Meyer MA, Baer JM, Knolhoff BL, Nywening TM, Panni RZ, Su X, et al. Breast and pancreatic cancer interrupt IRF8-dependent dendritic cell development to overcome immune surveillance. *Nat Commun* 2018;9:1250.
58. Cerami E, Gao J, Dogrusoz U, Gross BE, Sumer SO, Aksoy BA, et al. The cBio cancer genomics portal: an open platform for exploring multidimensional cancer genomics data. *Cancer Discov* 2012;2:401–4.
59. DiScala M, Najor MS, Yung T, Morgan D, Abukhdeir AM, Cobleigh MA. Loss of STAT6 leads to anchorage-independent growth and trastuzumab resistance in HER2+ breast cancer cells. *PLoS One* 2020;15: e0234146.
60. Tchakarska G, Sola B. The double dealing of cyclin D1. *Cell Cycle* 2020;19:163–78.
61. Lohani N, Singh HN, Moganty RR. Structural aspects of the interaction of anticancer drug Actinomycin-D to the GC rich region of hmgb1 gene. *Int J Biol Macromol* 2016;87:433–42.
62. Lohani N, Singh HN, Rajeswari MR. Assessment of binding properties of Actinomycin-D to 21nt DNA segment of hmgb1 gene promoter using spectroscopic and calorimetric techniques. *J Biomol Struct Dynam* 2018;36:504–11.
63. Lu D-F, Wang Y-S, Li C, Wei G-J, Chen R, Dong D-M, et al. Actinomycin D inhibits cell proliferations and promotes apoptosis in osteosarcoma cells. *Int J Clin Exp Med* 2015;8:1904–11.
64. Yun C, Lee JH, Park H, Jin YM, Park S, Park K, et al. Chemotherapeutic drug, adriamycin, restores the function of p53 protein in hepatitis B virus X (HBx) protein-expressing liver cells. *Oncogene* 2000;19:5163–72.
65. Lohani N, Narayan Singh H, Agarwal S, Mehrotra R, Rajeswari MR. Interaction of adriamycin with a regulatory element of hmgb1: spectroscopic and calorimetric approach. *J Biomol Struct Dynam* 2015;33:1612–23.

Supplementary Material: The online version of this article offers supplementary material (<https://doi.org/10.1515/jib-2021-0041>).